

Figure S1. Inhibition of AREG expression upon AREG siRNA transfection of AsPC-1 cells. (A) RT-qPCR analysis of AREG mRNA in siRNA- or control siRNA-transfected AsPC-1 cells. The data revealed a 30-65% reduction in AREG mRNA after AREG siRNA treatment compared with control siRNA. The bars represent the mean  $\pm$  SD of triplicate analyses (\* $P$ <0.05, \*\* $P$ <0.01). (B) ELISA of the conditioned medium of AsPC-1 cells transfected with AREG siRNAs revealing a substantial reduction in AREG upon siRNA transfection. The data revealed a 34-64% reduction in AREG protein after AREG siRNA treatment compared with control siRNA. AREG, amphiregulin; ELISA, enzyme-linked immunosorbent assay.

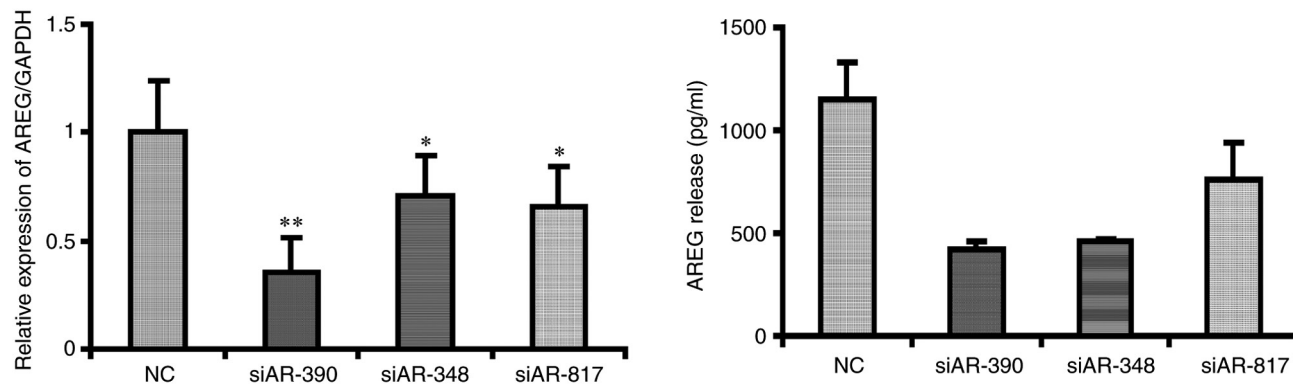




Figure S2. AREG mediates the EMT transition in BxPC-3 cells via the ERK/NF- $\kappa$ B signalling pathway. (A) Knockdown of AREG reduced migration in BxPC-3 cells (\*\* $P < 0.01$  vs. the control). (B) Knockdown of AREG in BxPC-3 cells increased the expression of E-cadherin and decreased the expression of  $\beta$ -catenin. Knockdown of AREG downregulated ERK and AKT phosphorylation. BxPC-3 cells transfected with AREG siRNA (siAR-390) or control siRNA (NC). The data represent the mean  $\pm$  SD of triplicate analyses (\* $P < 0.05$ , \*\* $P < 0.01$ ). (C) Western blotting was performed to examine the protein levels of vimentin in a panel of pancreatic cancer cell lines. (D) Knockdown of AREG reduced NF- $\kappa$ B/p65 nuclear accumulation. (a and d) The binding of the NF- $\kappa$ B/p65 antibody was visualized using a FITC-labelled secondary antibody. (b and e) The nuclei were counterstained with DAPI. (c and f) Merged images (original magnification,  $\times 1,000$ ). AREG, amphiregulin; EMT, epithelial-mesenchymal transition.

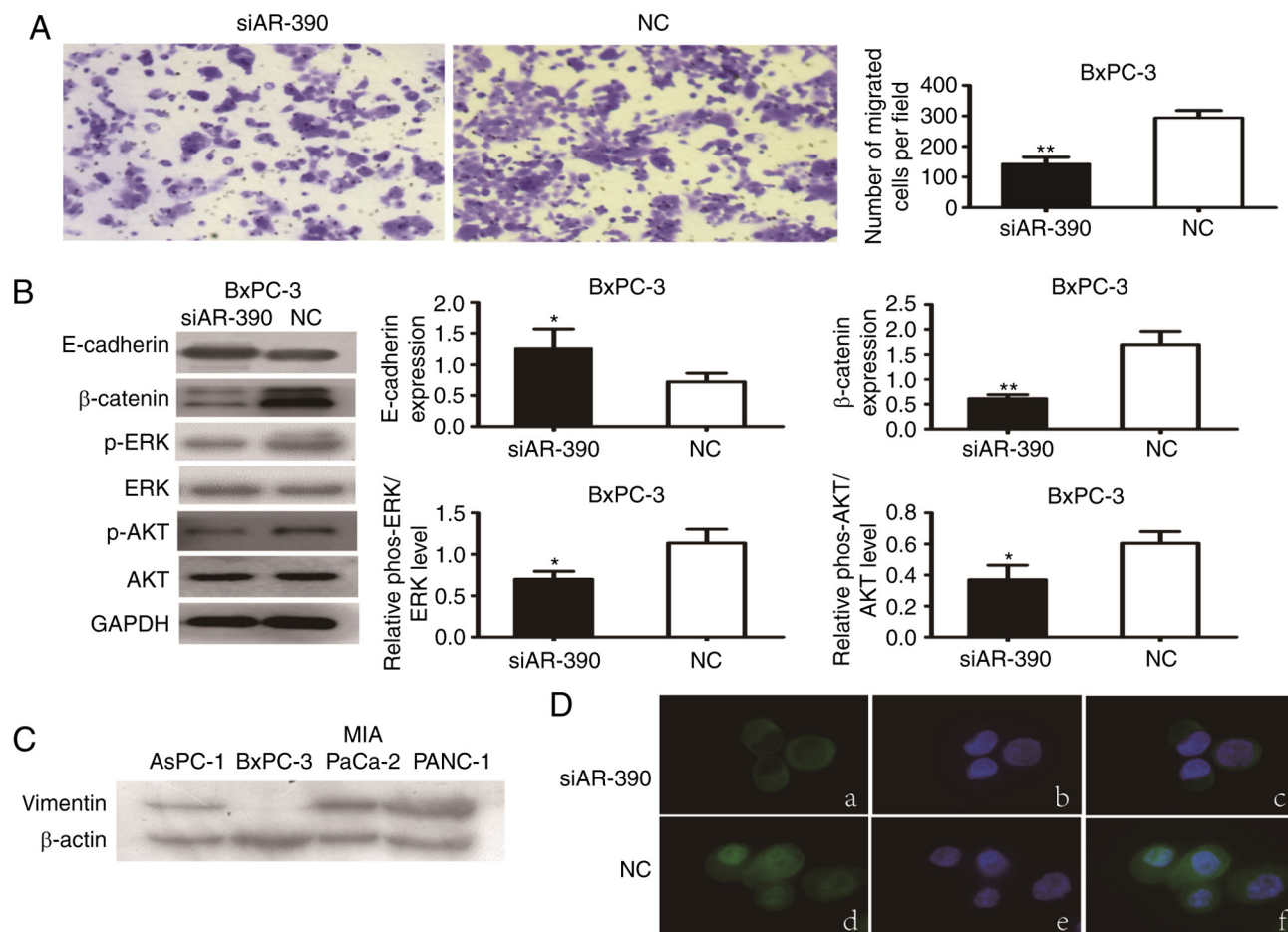




Figure S3. PSC-induced PANC-1 cell migration and invasion. (A) Immunofluorescence of EGFR and AREG in human pancreatic cancer tissue. (a) The binding of the EGFR antibody was visualized using an Alexa Fluor® 546-labelled secondary antibody. (b) The binding of the AREG antibody was visualized using an FITC-labelled secondary antibody. (c) The nuclei were counterstained with DAPI. (d) Merged image. (original magnification, x100). (B) Activated primary PSCs were observed by (a) phase contrast microscope and verified by (b) immunofluorescence staining of  $\alpha$ -SMA. Four PSCs were analysed for AREG expression by (c) RT-qPCR and (d) ELISA.

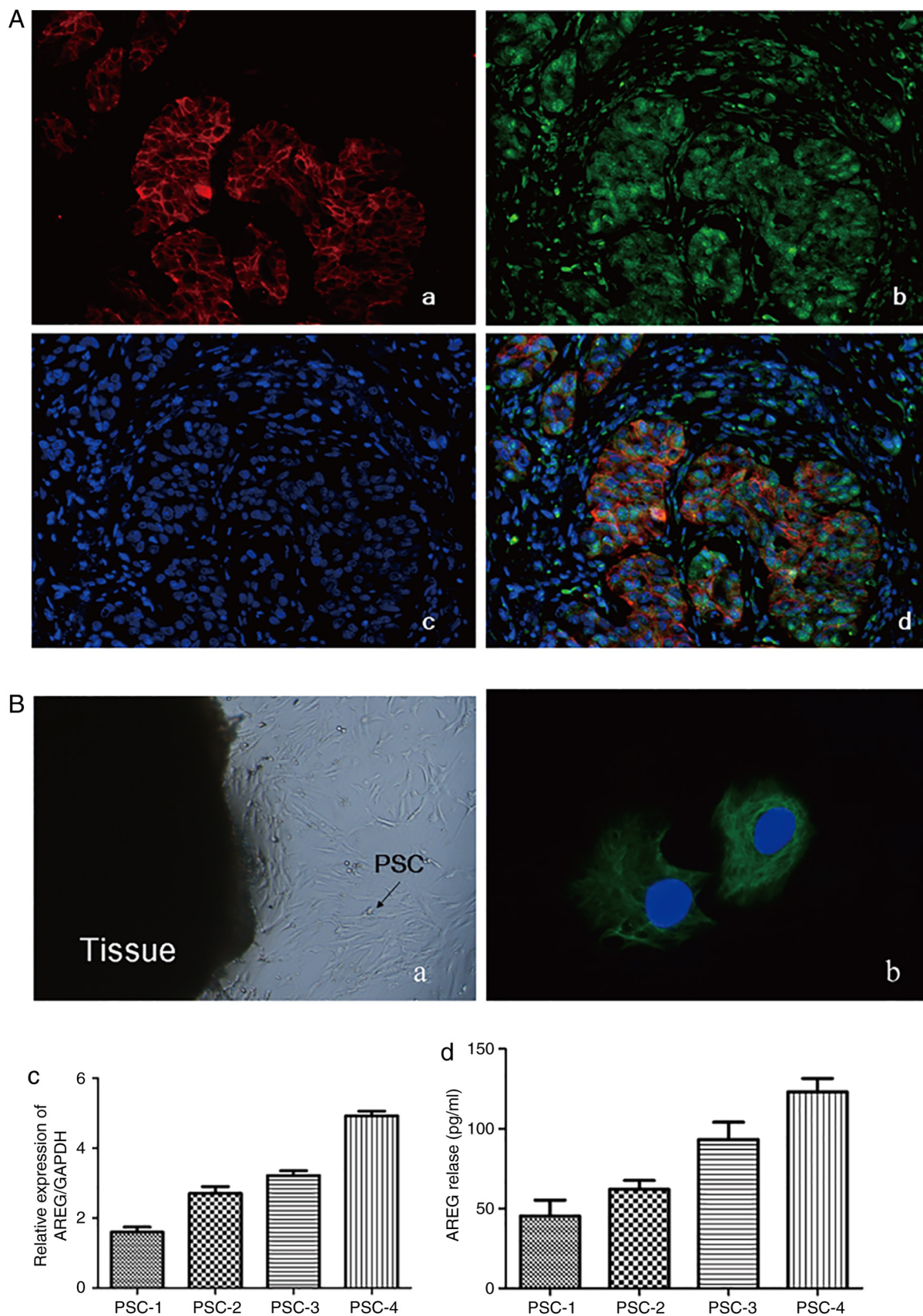




Figure S3. Continued. PSC-induced PANC-1 cell migration and invasion. (C) The effect of the PSCs in PANC-1 cell migration and invasion. The migratory and invasive abilities of the PANC-1 cells were significantly increased in the presence of the PSCs. The chemotactic effect of the PSCs on the PANC-1 cells could not be antagonized by the AREG-neutralizing antibody ( $P<0.05$ ;  $**P<0.01$ , vs. the control). PSCs, pancreatic stellate cells; EGFR, epidermal growth factor receptor; AREG, amphiregulin; ELISA, enzyme-linked immunosorbent assay.

